

Dynamic Response of Thin-walled Composite Beam-columns with Closed and Open Cross-sections

Jacek JANKOWSKI

*Technical University of Łódź,
Department of Strength of Materials and Structures
Stefanowskiego 1/15, 90-924 Łódź, Poland*

Received (25 October 2008)

Revised (30 October 2008)

Accepted (15 December 2008)

The paper deals with analysis of dynamic buckling of thin-walled beam-columns with various open and closed cross-sections subjected to lengthwise compressive rectangular pulse loading. The results were obtained with finite difference method and compared with finite elements method.

Keywords: Dynamic buckling, thin plates, orthotropic material

1. Introduction

Since 1960's, many works have described dynamic stability phenomenon as the response with respect to continuous structures i.e.: plates, shells, beams, columns, beam-columns, etc.. According to world literature, dynamic buckling can be determined only by using criterion of stability, because it appears without bifurcation point. One of the most famous is Volmir criterion [13], [9] at which the dynamic buckling stress occurs when the value of deflection is equal to plate thickness. Another criterion formulated by Budiansky and Hutchinson [3], [9] determines stability loss as a moment when small increase of load causes rapid growth of deflection. On the basis of plate stability analysis, Ari-Gur and Simonetta [2], [9] proposed four criteria introducing "load intensity" term corresponding to either loading or displacement pulse amplitude. Generally, they noticed that for high pulse intensities the dynamic buckling phenomenon is observed, but for low pulse intensities, quasi-static oscillations appear. However, this problem with respect to plate structures subjected to dynamic pulse loading is neglected in the world literature.

The approach to the solution of dynamic buckling phenomenon in this paper is based on the theory of orthotropic plates subjected to in-plane compression. The theory was adopted to obtain equilibrium equations for quasi-orthotropic beam-columns under compression. The solution was reached with finite difference method.

According to the general assumptions, the members are composed of thin plates made of isotropic or quasi-orthotropic material, subjected to axial compression of dynamic pulse loading. Structures are assumed as simply supported at the ends, but in case of open cross-sections, the beam-columns are simply supported at the lengthwise edges of plates 1 and 3, along axis x . In Fig. 1.a-b, members with closed section (square and trapezoidal section) are shown and in Fig. 1.c-d with open section (Z and C section). Pulse duration corresponds to period of free vibrations for the first static buckling mode.

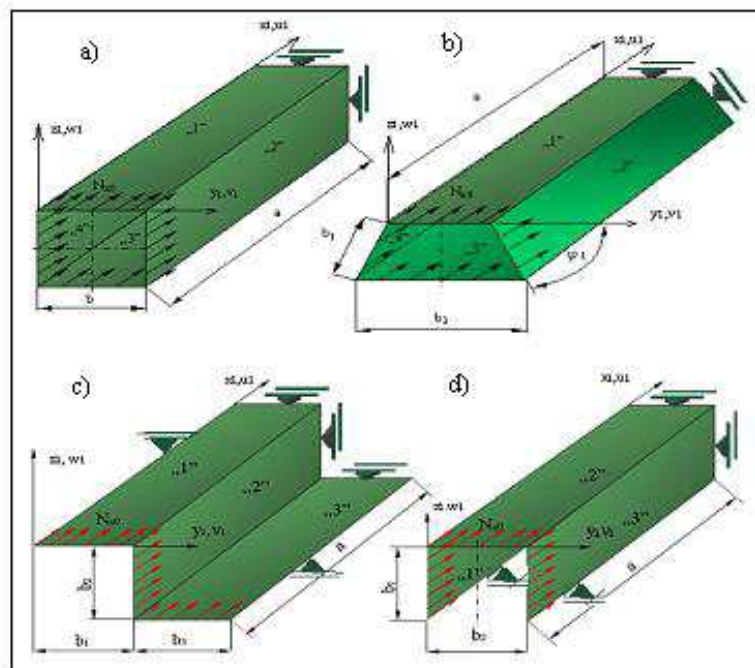


Figure 1 Types of analysed beam-columns: a) square, b) trapezoidal, c) Z-section, d) C-section. In figure, general dimensions and the way of loading are shown

2. Formulation of the problem

As it was described, every beam-column consists of plates. At one edge, i.e. $x = a$, constant amplitude of load is applied (Fig. 2). All edges at $x = 0$ and $x = a$ are assumed to be simply supported.

2.1. Basic relations of thin platss theory

Mathematical description of this problem can be reduced to formulate dynamic equilibrium equations taking into account boundary conditions. In addition, boundary conditions are assumed for joined edges of two plates.

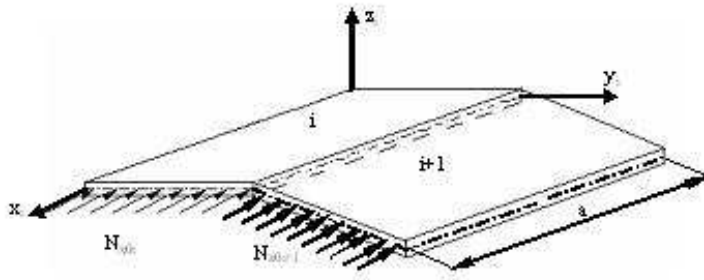


Figure 2 Scheme of loading with local coordinate system; N_{x0i}, N_{x0i+1} – loading amplitudes

For assumed model, membrane strains in the middle surface of single plate can be written as follows:

$$\begin{aligned}
 \varepsilon_{x^m} &= u_{,x} + \frac{1}{2}(v_{,x^2} + w_{,x^2}) \\
 \varepsilon_y^m &= v_{,y} + \frac{1}{2}w_{,y^2} \\
 \gamma_{xy}^b &= v_{,x} + u_{,y} + w_{,x}w_{,y}
 \end{aligned}
 \tag{1}$$

where: u, v, w – plate displacements in x, y, z directions respectively.

Forces and moments in the middle surface, corresponding to strains (??), can be written according to the following relations [8], [9]:

$$\begin{aligned}
 N_x &= K_{11}\varepsilon_x^b + K_{12}\varepsilon_y^b \\
 N_y &= K_{21}\varepsilon_x^b + K_{22}\varepsilon_y^b \\
 N_{xy} &= K_{66}\gamma_{xy}^b
 \end{aligned}
 \tag{2}$$

where: N_x, N_y, N_{xy} – sectional membrane forces,

$$\begin{aligned}
 M_x &= D_{11}w_{,xx} + D_{12}w_{,yy} \\
 M_y &= D_{21}w_{,xx} + D_{22}w_{,yy} \\
 M_{xy} &= D_{66}w_{,xy}
 \end{aligned}
 \tag{3}$$

where: M_x, M_y, M_{xy} – bending and twisting moments, D_{ij} – bending stiffness coefficients, K_{ij} – tension-compression stiffness coefficients.

Using Hamilton principle and formulas (1), (2) and (q3), the equilibrium equations can be express as follows:

$$N_{x,x} + N_{xy,y} = \rho h \frac{\partial^2 u(x,y,t)}{\partial t^2} \quad (4)$$

$$N_{xy,x} + N_{y,y} + (N_{x,x}v_{,x})_{,x} = \rho h \frac{\partial^2 v(x,y,t)}{\partial t^2} \quad (5)$$

$$M_{x,xx} + M_{y,yy} + 2M_{xy,xy} + (N_x w_{,x})_x + (N_y w_{,y})_y + (N_{xy} w_{,x})_y + (N_{xy} w_{,y})_x = \rho h \frac{\partial^2 w(x,y,t)}{\partial t^2} \quad (6)$$

The boundary conditions were considered for all the structure as simply supported at the edges:

- at the loaded ends, i.e. $x=a$:

$$w_i = 0; \quad u_{i,y} = 0; \quad v_i = 0; \quad \sum_i \int_0^{b_i} b_i N_x dy = \sum_i b_i N_x^0; \quad M_{x_i} = 0 \quad (7)$$

- at the unloaded ends, i.e. $x=0$:

$$w_i = 0; \quad u_i = 0; \quad v_i = 0; \quad M_{x_i} = 0 \quad (8)$$

Additionally, kinematic and static interaction conditions on the longitudinal edges of adjacent were written [8].

2.1.1. Initial conditions (at $t=0$)

- for displacements:

$$u_i(x,y,t=0) = v_i(x,y,t=0) = 0 \quad (9)$$

$$w_i(x,y,t=0) = w_{0i}(x,y) \quad (10)$$

- for displacements velocities:

$$\frac{\partial u_i(x,y,t=0)}{\partial t} = \frac{\partial v_i(x,y,t=0)}{\partial t} = \frac{\partial w_i(x,y,t=0)}{\partial t} = 0 \quad (11)$$

3. Short description of Finite Difference Method (FDM)

Solution of equilibrium equations (4), (5), (6) was performed using finite difference scheme [4], [10], [11] that was adopted to solve this problem. Replacing derivatives with corresponding difference quotients is connected with division of plates area on nodes that create grids. Exemplary grids are shown in Fig. 3.

In order to choose adequate grid type, it is necessary to satisfy the requirements as follows:

- increase of distance between nodes should improve coincidence of FDM,

- FDM should secure coincidence of implicit solution method,
- FDM should satisfy boundary conditions.

After the discretization, the system of algebraic equations is obtained in case of static phenomenon, but in case of dynamic phenomenon system of differential-difference equations is obtained.

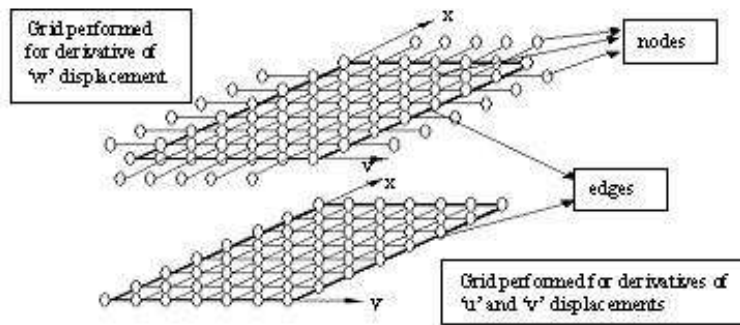


Figure 3 Types of grids performed by replacing derivatives with corresponding difference quotients

4. Analytical–numerical method of dynamic buckling problem solution

The system of differential–difference equations was solved using explicit Runge–Kutta method (fourth order method) [4] of derivative equations integration. Thanks to it, stability of solution could be achieved.

Results of calculations with FDM and finite elements method (FEM) [1] were compared and described.

In many works dealing with analytical methods, expansion of displacement field is often used (Koiter [6], Sridharan and Benito [12], Budiansky [3], Kolakowski [8]). In order to solve the equilibrium equations, a solution is predicted, i.e. buckling modes are approximated by trigonometric series. In the analytical–numerical method, the solution is obtained by solving derivative equations system, so the results of computations are obtained directly without prediction process. However, FDM requires long time of computations.

5. Results of computations

The analysis of the structures with open and close cross–sections was carried out on the basis of material data from Tab. 1–3 below, taking into account Tsai–Wu criterion [9] for quasi–orthotropic material:

$$F_1\sigma_{xk} + F_2\sigma_{yk} + F_6\tau_{xyk} + F_{11}\sigma_{xk}^2 + F_{22}\sigma_{yk}^2 + F_{66}\tau_{xyk}^2 + F_{12}\sigma_{xk}\sigma_{yk} = 1 \quad (12)$$

where:

$$F_1 = \frac{1}{X_r} - \frac{1}{X_c} F_2 = \frac{1}{Y_r} - \frac{1}{Y_c} F_6 = 0 F_{11} = \frac{1}{X_r X_c} F_{12} = -\frac{1}{2} \sqrt{F_{11} F_{22} F_{66}} = \frac{1}{S^2}$$

$X_{r,c}$ – tension (compression) strength in x direction

$Y_{r,c}$ – tension (compression) strength in y direction

S – shear strength.

The criterion determines the load-carrying capacity.

All the structures included initial imperfections of displacement ‘w’ amplitude equal to 0,01 plate thickness. As the most dangerous case of loading, the shape of pulse was assumed to be rectangular. Pulse duration corresponded to period of natural vibrations for buckling mode obtained for critical value of static load.

5.1. Geometric and material data

General dimensions and properties of analysed composite beam-columns are shown in Table 1 and material data in Tabs 2, 3 and 4. Layout of orthotropic plate layers was assumed according to $[0/90/90/0]_T$ configuration.

Table 1 General dimensions (see Fig. 1)

Type of cross-section	a [mm]	b [mm]	b ₁ [mm]	b ₂ [mm]	b ₃ [mm]	h [mm]	ϕ [deg]	T_0 [s]	N_{x0} [N/m]
squared	500	100	-	-	-	1	90	0,0047	6253
trapezoidal	500	-	100	100	200	1	60	0,011	2309
C ₁	500	-	100	40	-	1	90	0,0028	9514
C ₂	500	-	100	100	-	1	90	0,0048	6253
Z ₁	500	-	40	100	40	1	90	0,0029	9513
Z ₂	500	-	100	100	100	1	90	0,0048	6250

where:

N_{xcr} – critical load of static loss of stability obtained from FDM,

T_0 – period of natural vibrations obtained from FDM

Table 2 Material data [5]; type of material: Kevlar – data corresponds to single layer

Material type	density [kg/m ³]	E_x [MPa]	E_y [MPa]	G_{xy} [MPa]	ν_{xy}	h_i [mm]
quasi-orthotropic	1280	76000	5500	2100	0,34	0,25
isotropic	7800	200000	200000	77000	0,3	-

where: i – number of layers.

Table 3 Strength material data [5] (from tension, compression and shear tests)

X_r [MPa]	X_c [MPa]	Y_r [MPa]	Y_c [MPa]	S [MPa]
1400	235	12	53	34

Results of calculations are shown in Tab. 4 .

A detailed analysis for single layer has shown that load amplitude limit is equal to 182,5 [kN/m] and corresponding the maximum stress value (in external layers of

Table 4 Load-carrying capacity N_{x0lim}

N_{x0lim} [kN/m]	σ_{xlim} [MPa]	σ_{ylim} [MPa]
182,5	-339,9	-7,2

single plate) is equal to nearly 340 [MPa] (it is grater than X_c). It follows that, if load amplitude is greater than load limit, the external layers are destroyed.

6. Comparison of results

The beam-columns with open and closed cross-section and made of different types of material were investigated. The analysis was based on determining critical dynamic load amplitude $N_{x0\ dyn}$ from the curves of dynamic load factor ($DLF = N_{x0\ dyn}/N_{x0}$) versus maximal plate deflection w_{max} using Budiansky-Hutchinson criterion of stability adopted to the dynamic buckling of plate structures. It means the structure will loose the dynamic stability if the critical value of coefficient DLF is reached. Pulse duration $T_0 = 2\pi/\omega_1$ (ω_1 [rad/s] – frequency of natural vibrations) was assumed to be equal to period of natural vibrations for buckling mode corresponding to static critical load.

a)

b)

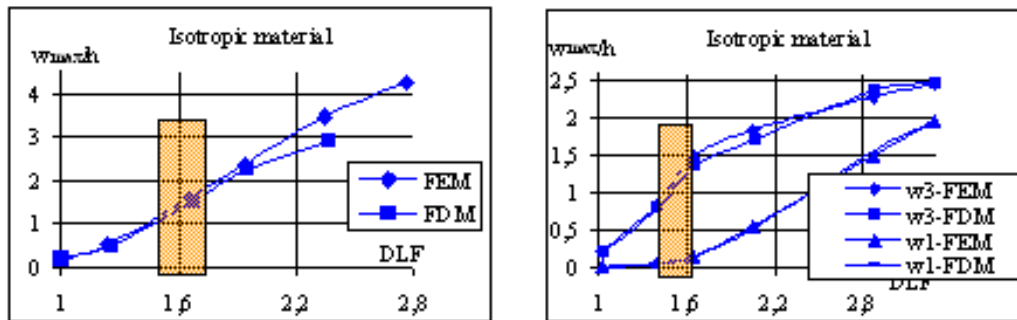


Figure 4 a) – DLF factor vs. w_{max}/h for square section, b) – DLF factor vs. w_{max}/h for trapezoidal section

On the curves, the dynamic instability area has been marked with rectangles. In Figs 4-6 the curves for isotropic material were shown and in Figs 7-10 – for quasi-orthotropic material.

For beam-column with square section, the critical value of DLF factor obtained with the FEM and FDM is similar and equals 1.6 for isotropic material (Fig. 4a)

and 1.72 for quasi-orthotropic material (Fig. 7a). The stability loss appears in all plates at the same moment. Critical DLF factor for trapezoidal section for isotropic material equals 1.5 (Fig. 4b) and for other material – 1.75 (Fig. 7b).

a) b)

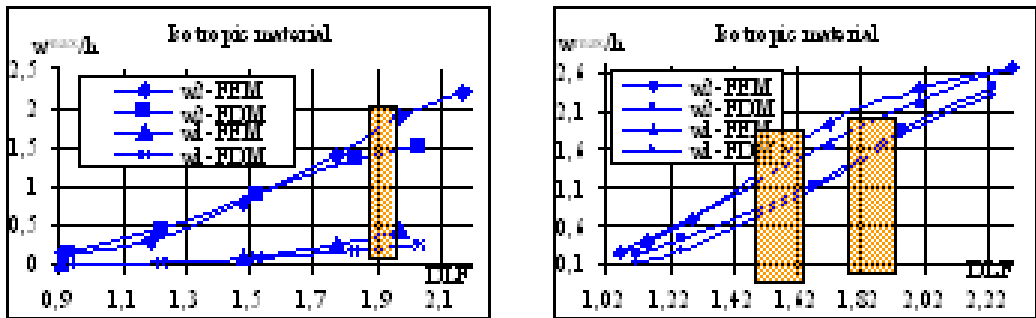


Figure 5 a) – DLF factor vs. w_{max}/h for C_1 section, b) – DLF factor vs. w_{max}/h for C_2 section

a) b)

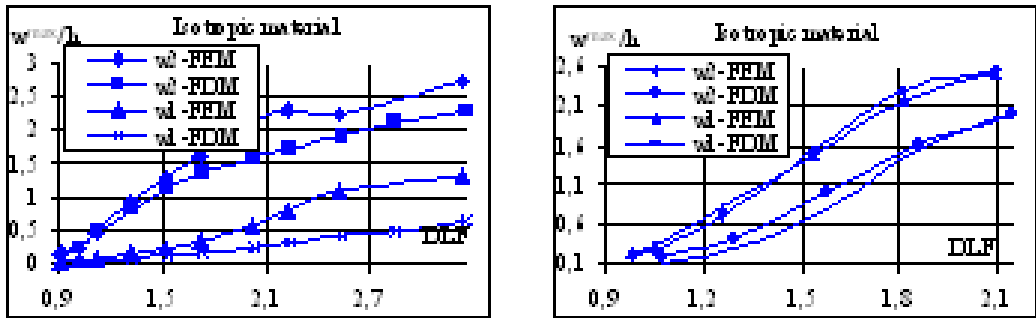


Figure 6 a) – DLF factor vs. w_{max}/h for Z_1 section, b) – DLF factor vs. w_{max}/h for Z_2 section

It can be noticed that values of DLF obtained for squared and trapezoidal cross-sections depending on material type are similar, but in case of trapezoidal section, the widest plate initiates the stability loss. In case of quasi-orthotropic beam-column with open C_1 cross-section, dynamic buckling appears when critical $DLF =$

1.4 (FDM result) or $DLF = 1.55$ (FEM result) for plate 2 (Fig. 8) and for C_2 section critical $DLF = 1.7$ (Fig. 9a). For isotropic material (C_1 section) critical value of $DLF = 1.55$ (FDM result) or $DLF = 1.85$ (FEM result) (Fig. 5a) and for C_2 section – 1.8 (FDM result) or 1.53 (FEM result) (Fig. 5b).

a)

b)

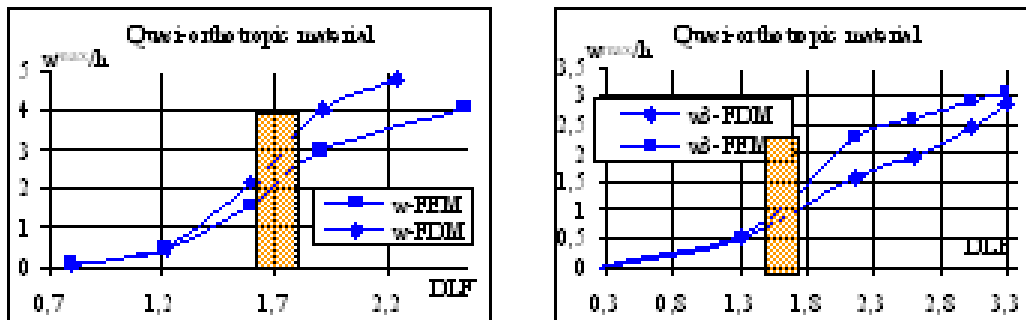


Figure 7 a) – DLF factor vs. w_{max}/h for square section , b) – DLF factor vs. w_{max}/h for trapezoidal section

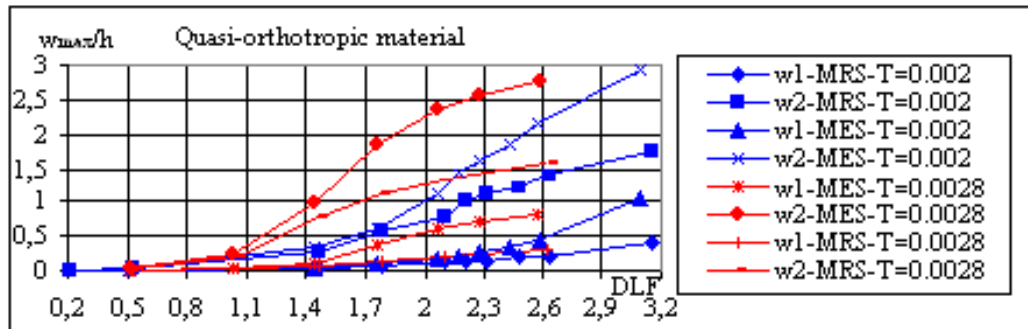


Figure 8 DLF factor vs. w_{max}/h for C_1 section - the influence of pulse duration on the critical DLF value; $T_0 = 0,0028$ s (see Tab. 1)

For quasi-orthotropic beam-column with open Z_1 cross-section critical DLF value equals 1.65 for plate 2 and for Z_2 section critical $DLF = 1.75$. For isotropic material (Z_1 section) critical value of $DLF = 1.3$ (FDM result) or $DLF = 1.6$ (FEM result) and for Z_2 section – 1.7 (FDM result) or 1.55 (FEM result) for plate 2 and 1.53 (FDM result) or 1.4 (FEM result) for plates 1 and 3.

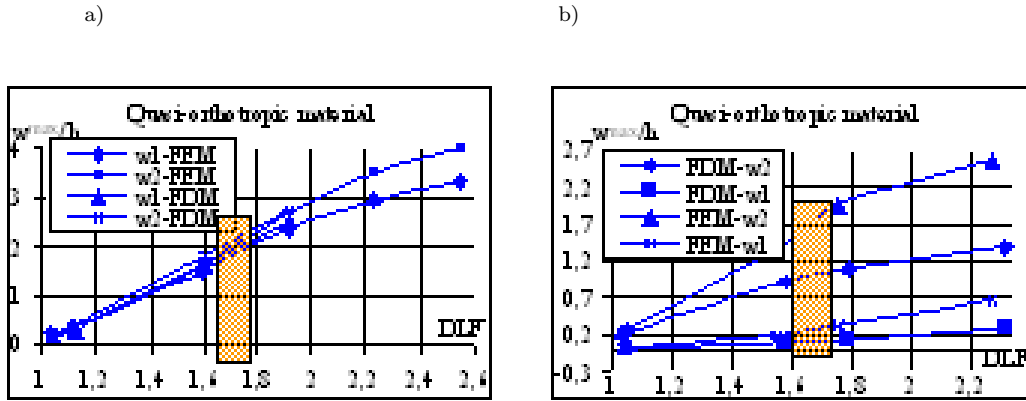


Figure 9 a) – DLF factor vs. w_{max}/h for C_2 section , b) – DLF factor vs. w_{max}/h for Z_1 section

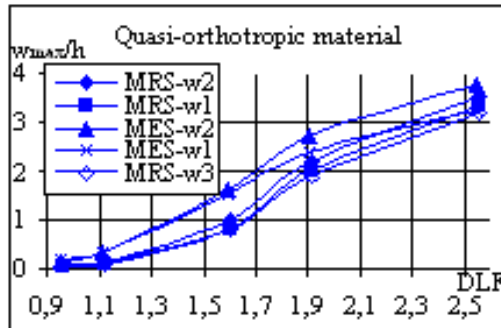


Figure 10 DLF factor vs. w_{max}/h for Z_1 section

Detailed analysis has shown that results obtained with both methods can differ significantly, especially for beam–columns with open cross–sections. The reason is greater degrees of freedom number that was assumed in numerical FEM models. Thanks to it, these models could take into consideration change of buckling modes.

7. Conclusions

On the basis of the results, the following conclusions have been drawn:

- Method of solution, for assumed level of difficulty of used theory, gives generally good agreement between results of FEM for static as well as dynamic

loading amplitude. The best agreement was obtained for beam-column with square cross-section.

- Threshold of amplitude loading depends on type of structure, material and nature of loading (static, dynamic).
- Phenomenon of dynamic buckling appears, when the duration of pulse loading is comparable to the period of natural vibrations (number of wavelength $m > 1$) corresponding to the buckling mode for the lowest critical force.
- Interaction and change of buckling mode does not appear in structure with square cross-section but with open cross-section, for assumed level assumptions and simplifications used theory. As it was shown, the beam-column with trapezoidal cross-section can undergo less significant global flexural mode of buckling.
- The local buckling usually appears in the short-length beam-columns with open cross-section. We should not consider the global mode of buckling as Euler buckling, because the boundary conditions limit this kind of buckling. In aspect of dynamic buckling, less significant mode of torsion buckling appear in analyzed structures.

References

- [1] **ANSYS Theory Reference**, Release 5.6, www.ansys.com,
- [2] **Ari-Gur, J. and Simonetta, S.R.**: Dynamic pulse buckling of rectangular composite plates, *Composites*, Part B, 28B, p. 301-308, **1997**.
- [3] **Budiansky, B. and Hutchinson J.W.**: Dynamic buckling of imperfection-sensitive structures, *Proceed. XIth Internat. Congr. Appl. Mech. Berlin*, p. 636-651, **1964**.
- [4] **Collatz, L.**: Numerical methods of solution of differential equations system, Warsaw **1960**.
- [5] **German, J.**: The fundamentals of mechanics of fibre composites, Script of Technical University of Krakow, Krakow **2001**.
- [6] **Koiter, W. T.**: Elastic stability and post-buckling behaviour. In: *Proceedings of the Symposium on Nonlinear Problems, Univ. of Wisconsin Press, Wisconsin*, p. 257-275, **1963**.
- [7] **Kořakowski, Z. and Kowal-Michalska K.**: Selected problems of instabilities in composite structures, Łódź, p. 16-35, **1999**.
- [8] **Kořakowski, Z. and Teter, A.**: Interactive buckling of thin-walled beam-columns with intermediate stiffeners or/and variable thickness, *International Journal of Solids and Structures*, 37, (24), 3323-3344, **2000**.
- [9] **Kowal-Michalska, K.**: Dynamic stability of composed plate structures, (ed.), Warsaw, **2007**.
- [10] **Marczuk, G. I.**: Numerical analysis of applied physics phenomena, Warsaw **1983**.
- [11] **Pietrzak, J., Rakowski, G. and Wrzesniowski, K.**: Matrix analysis of steel structures, Warsaw, **1986**.
- [12] **Sridharan, S. and Benito, R.**: Columns static and dynamic interactive buckling, *Journal of Engineering Mechanics*, ASCE 110-1, p.49-65, **1984**.
- [13] **Volmir, A. S.**: Nonlinear Dynamics of Plates and Shells, *Science*, Moscow, **1972** (in Russian).

